



ARTICLE

Sustained over-expression of calpain-2 induces age-dependent dilated cardiomyopathy in mice through aberrant autophagy

Xiao-yun Ji^{1,2,3}, Dong Zheng⁴, Rui Ni^{2,3}, Jin-xi Wang⁵, Jian-qiang Shao⁶, Zer Vue⁷, Antentor Hinton Jr.⁷, Long-Sheng Song⁵, Guo-Chang Fan⁸, Subrata Chakrabarti³, Zhao-liang Su¹ and Tian-qing Peng^{2,3,9}

Calpains have been implicated in heart diseases. While calpain-1 has been detrimental to the heart, the role of calpain-2 in cardiac pathology remains controversial. In this study we investigated whether sustained over-expression of calpain-2 had any adverse effects on the heart and the underlying mechanisms. Double transgenic mice (Tg-Capn2/tTA) were generated, which express human CAPN2 restricted to cardiomyocytes. The mice were subjected to echocardiography at age 3, 6, 8 and 12 months, and their heart tissues and sera were collected for analyses. We showed that transgenic mice over-expressing calpain-2 restricted to cardiomyocytes had normal heart function with no evidence of cardiac pathological remodeling at age 3 months. However, they exhibited features of dilated cardiomyopathy including increased heart size, enlarged heart chambers and heart dysfunction from age 8 months; histological analysis revealed loss of cardiomyocytes replaced by myocardial fibrosis and cardiomyocyte hypertrophy in transgenic mice from age 8 months. These cardiac alterations closely correlated with aberrant autophagy evidenced by significantly increased LC3BII and p62 protein levels and accumulation of autophagosomes in the hearts of transgenic mice. Notably, injection of 3-methyladenine, a well-established inhibitor of autophagy (30 mg/kg, i.p. once every 3 days starting from age 6 months for 2 months) prevented aberrant autophagy, attenuated myocardial injury and improved heart function in the transgenic mice. In cultured cardiomyocytes, over-expression of calpain-2 blocked autophagic flux by impairing lysosomal function. Furthermore, over-expression of calpain-2 resulted in lower levels of junctophilin-2 protein in the heart of transgenic mice and in cultured cardiomyocytes, which was attenuated by 3-methyladenine. In addition, blockade of autophagic flux by bafilomycin A (100 nM) induced a reduction of junctophilin-2 protein in cardiomyocytes. In summary, transgenic over-expression of calpain-2 induces age-dependent dilated cardiomyopathy in mice, which may be mediated through aberrant autophagy and a reduction of junctophilin-2. Thus, a sustained increase in calpain-2 may be detrimental to the heart.

Keywords: calpain-2; dilated cardiomyopathy; heart dysfunction; autophagy; junctophilin-2; 3-methyladenine

Acta Pharmacologica Sinica (2022) 43:2873–2884; <https://doi.org/10.1038/s41401-022-00965-9>

INTRODUCTION

Calpains belong to a family of calcium-dependent neutral cysteine proteases [1]. Fifteen calpain isoforms have been identified in mammals, among which calpain-1 and calpain-2 are ubiquitously expressed and well-studied [2]. Both calpain-1 and calpain-2 consist of a large catalytic subunit CAPN1 (encoded by *Capn1*) and CAPN2 (encoded by *Capn2*), respectively, and a regulatory small subunit CAPNS1 (or CAPN4) encoded by *Capns1* (or *Capn4*). CAPNS1 is required for the assembly and activation of calpain-1 and calpain-2 as deletion of *Capns1* abolishes their activities [3]. Calpain participates in a wide range of physiological and pathological processes [4–6]. However, studies have found that calpain-1 null mice grow normally whereas calpain-2 deficient mice are embryonically lethal, suggesting that calpain-2 is required for development and/or important physiological functions [7, 8]. Numerous

evidences have shown that calpain activation plays a critical role in heart diseases under various pathological conditions including myocardial ischemia/reperfusion injury [4, 9, 10], myocardial infarction [11], diabetes [6], sepsis [12, 13], angiotensin II-induced cardiac hypertrophy [14] and heart failure [15, 16], etc. In most contexts, calpain-1 activation is detrimental to the heart and transgenic over-expression of calpain-1 in cardiomyocytes was sufficient to induce dilated cardiomyopathy in mice [4, 16]. In contrast, calpain-2 has been reported to induce death and survival signaling, and the role of calpain-2 remains controversial in cardiac pathology [17–19].

Increased calpain-2 activation was suggested to be associated with increased susceptibility to isoproterenol-induced cardiomyocyte apoptosis in tail-suspended rats [20], cardiomyocyte remodeling induced by overload and isoproterenol [21], and complex I

¹International Genome Center, Jiangsu University, Zhenjiang 212013, China; ²Lawson Health Research Institute, London Health Sciences Centre, London, ON N6A 5W9, Canada; ³Department of Pathology and Laboratory Medicine, Western University, London, ON N6A 5C1, Canada; ⁴Centre of Clinical Laboratory, the First Affiliated Hospital of Soochow University, Suzhou 215006, China; ⁵Division of Cardiovascular Medicine, Department of Internal Medicine, Abboud Cardiovascular Research Center, Carver College of Medicine, University of Iowa, Iowa City, IA 52242, USA; ⁶Central Microscopy Research Facility, University of Iowa, Iowa City, IA 52242, USA; ⁷Department of Molecular Physiology and Biophysics, Vanderbilt University, Nashville, TN 37232, USA; ⁸Department of Pharmacology and Systems Physiology, University of Cincinnati College of Medicine, Cincinnati, OH 45267, USA and ⁹Department of Medicine, Western University, London, ON N6A 5W9, Canada
Correspondence: Zhao-liang Su (szl30@ujs.edu.cn) or Tian-qing Peng (tpeng2@uwo.ca)

Received: 27 December 2021 Accepted: 24 July 2022

Published online: 19 August 2022

inactivation and mPTP opening in the rat heart following ischemia/reperfusion [10, 22]. It was recently reported that inhibition of calpain-2 prevented apoptosis induced by activation of chemoattractant receptor-homologous molecule expressed on T helper type-2 cells (CRTH2) in cardiomyocytes [23]. In striking contrast, we have shown that increased calpain-2 attenuated doxorubicin-induced apoptosis in cardiomyocytes and protected against cardiac injury in mouse models of doxorubicin-induced acute and chronic cardiotoxicity [17]. Similar cardio-protection of calpain-2 up-regulation was also observed in heat stress-induced injury [19]. These previous studies indicate that the roles of calpain-2 (beneficial versus detrimental) may be dependent on pathological conditions. Notably, we recently reported that transgenic mice with constitutive over-expression of calpain-2 restricted to cardiomyocytes displayed normal heart structure and function in young mice (by age 4 months), suggesting that a relative short-term increase in cardiomyocyte calpain-2 may not be sufficient to cause damage to the heart [17]. Given our recent evidence that calpain-2 specifically cleaves junctophilin-2, an important structural protein organizing cardiac dyads, at the same site as calpain-1 but with less efficacy [24], sustained up-regulation of calpain-2 may be detrimental to the heart. Nevertheless, the role of calpain-2 in cardiac pathogenesis requires further investigations.

In this study, we took the advantage of the availability of transgenic mice with cardiomyocyte-specific calpain-2 over-expression to examine whether sustained over-expression of calpain-2 had any adverse effects in the heart and the underlying mechanisms.

MATERIALS AND METHODS

Animals

This investigation conforms to the Guide for the Care and Use of Laboratory Animals published by the US National Institutes of Health (NIH Publication, 8th Edition, 2011). All experimental procedures were approved by the Animal Use Subcommittee at the Western University, Canada. Breeding pairs of C57BL/6 mice were purchased from the Jackson Laboratory. Transgenic mice with cardiomyocyte specific over-expression of tetracycline transactivator (Tg-tTA) were kindly provided by Dr. Jeffrey Robbins [25] (Department of Pediatrics, Division of Molecular Cardiovascular Biology, The Children's Hospital Research Foundation, Cincinnati, OH 45229-3039, USA) and transgenic mice with human *Capn2* expression driven by tTA inducible mouse α -myosin heavy chain (MHC) promoter (Tg-Capn2) were generated as described [17]. Double transgenic mice (Tg-Capn2/tTA) were produced by crossing Tg-Capn2 mice with Tg-tTA mice, which express human CAPN2 restricted to cardiomyocytes as described in our recent report [17]. All animals were housed in a temperature and humidity-controlled facility at a 12-h light and dark cycles with water and food *ad libitum*.

Experimental protocols

Male Tg-Capn2/tTA mice and their littermate controls including wild-type, Tg-tTA, and Tg-Capn2 male mice were subjected to echocardiography at age 3, 6, 8 and 12 months, and their heart tissues and sera were collected for further analyses.

Male Tg-Capn2/tTA mice and their littermate controls were injected with 3-methyladenine (3-MA in 100–150 μ L of saline, 30 mg/kg, i.p., catalog number: M9281, Sigma–Aldrich Canada Co., Oakville, ON, Canada), an inhibitor of phosphatidylinositol 3-kinase widely used to inhibit autophagy, or the same volume of saline as Vehicle once every 3 days starting from age 6 months for a total of 2 months. Accordingly, they were subjected to various experiments at age 8 months.

Echocardiography

Mice were anesthetized with inhaled isoflurane (1%) and imaged using a 40 MHz linear array transducer attached to a preclinical

ultrasound system (Vevo 2100, FUJIFILM Visual Sonics, Toronto, ON, Canada) with a nominal in-plane spatial resolution of 40 μ m (axial) \times 80 μ m (lateral). M-mode and 2-D parasternal short-axis scans (133 frames/s) at the level of the papillary muscles were employed to assess changes in left ventricular (LV) end-systolic inner diameter, LV end-diastolic inner diameter, LV anterior and posterior wall thickness in end-diastole and end-systole, and fractional shortening (FS).

Histological analysis

Heart tissues were fixed in 4% paraformaldehyde (catalog number: 158127, Sigma-Aldrich Canada Co., Oakville, ON, Canada) at 4 °C for 48 h and then routinely processed, wax-embedded and sectioned. After processing, the tissue sections (5 μ m thick) were stained with hematoxylin (catalog number: H9627, Sigma–Aldrich Canada Co., Oakville, ON, Canada) and eosin (catalog number: E4009, Sigma–Aldrich Canada Co., Oakville, ON, Canada) (H&E), Texas RedTM-X Conjugated Wheat Germ Agglutinin (WGA, catalog number: W21405, Thermo Fisher Scientific, Markham, ON, Canada) for cardiomyocyte cross-sectional areas, or a saturated solution of picric acid containing 1% Sirius red (catalog number: 365548, Sigma-Aldrich Canada Co., Oakville, ON, Canada) for collagen deposition measurement as described previously [26]. Nuclei were stained by Hoechst 33342 (catalog number: H1399, Invitrogen, Burlington, ON, Canada). The signals were visualized by fluorescent microscopy and photographed. Cardiomyocyte cross-sectional areas were determined by the software ImageJ. The collagen deposition was determined by computer-assisted morphometry (Image-Pro Plus Version 6.0, Media Cybernetics, Inc., Rockville, MD, USA) and presented as the ratio of collagen deposition area over total area in heart sections. For each sample, at least 30 fields were analyzed.

Transmission electron microscopy

After overnight fasting, Tg-Capn2/tTA mice and their littermate controls (male at age 8 months) were humanely euthanized. Heart tissues were freshly excised and immediately washed with ice-cold buffer. As previously described [27, 28], samples were processed at the University of Iowa Microscopy Core Facility. The number of autophagosomes per μ m² was analyzed.

Cardiomyocyte cultures and adenoviral infection

The neonatal cardiomyocytes were prepared from mice born within 24 h after decapitation and cultured according to methods we described previously [29]. The rat cardiomyocyte-like H9c2 cells were purchased from the American Type Culture Collection (ATCC) and cultured H9c2 cells were employed within 10 generations.

Cardiomyocytes were infected with an adenoviral vector containing rat *Capn2* (Ad-Capn2, Vector Biolabs, Malvern, PA, USA) or human LGALS1 fused with green fluorescence protein (Ad-hLGALS1/GFP, SignaGen Laboratories, Rockville, MD, USA) at a multiplicity of infection of 100 plaque forming units/cell. An adenoviral vector containing hemagglutinin (Ad-HA, Vector Biolabs, Malvern, PA, USA) served as a control. Adenovirus-mediated gene transfer was performed as previously described [29].

Confocal microscopy

H9c2 cells were seeded in glass bottom culture dishes (35 mm petri dish, 14 mm microwell). Seventy-two hours after infection of adenoviral vectors (Ad-Capn2, Ad-hLGALS1/GFP or Ad-HA), H9c2 cells were fixed with freshly prepared 4% paraformaldehyde. Nuclei were stained using Hoechst 33342. Confocal microscopy was performed to capture the fluorescent signals using the Olympus FV 1000 laser-scanning microscope equipped with

a 63×, 1.3 NA oil immersion objective at a sampling rate of 0.7 s/frame as described previously [12].

Lysosomal pH measurement

Cardiomyocytes were incubated with LysoSensor yellow/blue DND-160 (1 μM, catalog number: L7545, Invitrogen, Burlington, ON, Canada) for 5 min at 37 °C. The LysoSensor dye is a ratiometric probe that produces yellow fluorescence in acidic environments but changes to blue fluorescence in neutral environments. The fluorescent signals were determined using a fluorescence spectrophotometer with excitation of 340 and 355 nm. The ratio of emission (460/535 nm) was then calculated as an indicator of lysosomal pH for each sample.

Real-time reverse transcription PCR

Total RNA was extracted from heart samples using TRIzol Reagent (catalog number: T9424, Sigma–Aldrich Canada Co., Oakville, ON, Canada) following the manufacturer's instructions. Real-time reverse transcription PCR was performed to analyze the mRNA levels of *ANP*, *β-MHC*, *collagen-I*, *collagen-III* and *Gapdh* as previously described [26]. The sequences of the primers for the *ANP*, *β-MHC*, *collagen-I*, *collagen-III* and *GAPDH* were as follows. *ANP*: 5'-CTGCTAGACCACCTGGAGGA-3' (forward), 5'-AAGCTGTTCAGCCTAGTCC-3' (reverse); *β-MHC*: 5'-TGCAAAGGCTCCAGTCTGAGGGC-3' (forward), 5'-GCCAACCAACCTGTCCAAGTTC-3' (reverse); *collagen-I*: 5'-ACGGCTGCACGAGTCACAC-3' (forward), 5'-GGCAGGCGGGAGGTCTT-3' (reverse); *collagen-III*: 5'-GTTCTAGAGGATGGCTGTACTAAACACA-3' (forward), 5'-TTGCTTGCGTGTGGATATTC-3' (reverse); *Gapdh*: 5'-CAGACTCTGCGATGTTTCCA-3' (forward), 5'-GCCTGAGCACTCCAGAAAC-3' (reverse).

Western blot analysis

Heart tissues and cardiomyocytes were lysed and the protein concentrations in their lysates were determined using the DC protein assay kit (catalog number: 5000111, Bio-Rad Laboratories (Canada) Ltd., Mississauga, ON, Canada). A total of 40 μg of total proteins were subjected to SDS-polyacrylamide gel electrophoresis. After the proteins were transferred to PVDF membranes (catalog number: 1620177, Bio-Rad Laboratories (Canada) Ltd., Mississauga, ON, Canada), Western blot analysis was conducted to determine the protein levels of interest using specific antibodies. Primary antibodies against LC3B (catalog number: 2775 S, 1:1000 dilution, Cell Signaling Technology, Danvers, MA, USA), p62 (catalog number: 5114 S, 1:1000 dilution, Cell Signaling Technology, Danvers, MA, USA), JPH2 (catalog number: 40–5300, 1:1000 dilution, Invitrogen Canada Inc., Burlington, ON, Canada; or custom made by Pacific Immunology Inc., Ramona, CA, USA), CAPN2 (catalog number: 2539 S, 1:1000 dilution, Cell Signaling Technology, Danvers, MA, USA), Cathepsin B (catalog number: 31718, 1:1000 dilution, Cell Signaling Technology, Danvers, MA, USA) and GAPDH (catalog number: 2118 S, 1:1000 dilution, Cell Signaling Technology, Danvers, MA, USA) were employed. Horseradish peroxidase (HRP)-conjugated goat anti-mouse IgG (H + L) secondary antibody was purchased from Bio-Rad (catalog number: 1706516, Hercules, CA, USA), and HRP-conjugated goat anti-rabbit IgG (H + L) from Bio-Rad (catalog number: 1706515, Hercules, CA, USA).

Measurement of troponin I in serum

Troponin I in serum was measured using a commercially available kit from Biomatik (catalog number: EKN49012, Kitchener, ON, Canada) following the manufacturer's instructions.

Statistical analysis

The data are expressed as the mean ± SD. Two-way ANOVA followed by the Newman-Keuls test was performed for multi-group comparisons. Unpaired Student's *t*-test was used for comparison between 2 groups. A *P* value of less than 0.05 was considered significant.

RESULTS

Sustained calpain-2 over-expression induces age-dependent dilated cardiomyopathy in transgenic mice

Although we have reported that transgenic over-expression of calpain-2 did not induce abnormal cardiac phenotypes in mice by age 4 months [17], it remains to be determined whether sustained up-regulation of calpain-2 for a longer period of time had any adverse effects on the heart. To address this, we monitored transgenic Tg-Capn2/tTA mice and their littermate controls from age 3 months to 12 months. The littermate controls represented a mixture of wild-type, Tg-Capn2 and Tg-tTA mice (Supplementary Table S1) as we found that they were normal without any cardiac phenotypes [17]. No death was observed in both Tg-Capn2/tTA mice and their control littermates by age 12 months. Echocardiographic analysis revealed normal myocardial function as determined by EF% and FS% in transgenic Tg-Capn2/tTA mice at age 3 months, which is consistent with our recent report [17]; however, the transgenic Tg-Capn2/tTA mice began to display mild myocardial dysfunction at age 6 months and a dramatic decline in myocardial function at ages 8 and 12 months when compared with their littermate controls (Fig. 1a–c). The decline in myocardial function was well correlated with myocardial pathological changes as evidenced by loss of cardiomyocytes and replacement of fibrosis (Fig. 1d) and adverse myocardial remodeling as determined by increases in cardiomyocyte size (Fig. 1d, e) and collagen depositions in transgenic Tg-Capn2/tTA mice compared with their littermate controls at ages 8 and 12 months (Fig. 1d, f). The littermate control mice exhibited normal myocardial function and no abnormalities in cardiac histology by age 12 months (Fig. 1a–f). To provide evidence of dilated heart failure in transgenic Tg-Capn2/tTA mice, we showed that the transgenic Tg-Capn2/tTA mice had a much bigger heart and their heart chambers were enlarged at age 8 months as compared to those in their littermate controls (Fig. 1g, h, Table 1). Histological analysis demonstrated lung congestion in transgenic Tg-Capn2/tTA mice, additional evidence supporting heart failure (Fig. 1i). Taken together, sustained over-expression of calpain-2 induced age-dependent dilated heart failure in transgenic mice.

Calpain-2 over-expression instigates age-dependent aberrant autophagy in transgenic mice

To understand the underlying mechanisms by which sustained over-expression of calpain-2 induced dilated heart failure, we determined autophagy in the heart as calpain has been implicated in keeping normal autophagic activity and participating in aberrant autophagy while autophagy is essential for cardiac homeostasis [22, 30, 31]. As shown in Fig. 2a, both LC3BII (an indicator of autophagy induction, Fig. 2a1, a2) and p62 (an indicator of autophagic flux activity, Fig. 2a1, a3) remained unaltered in littermate control mouse hearts with age (from age 3 months to 12 months). The levels of LC3BII and p62 did not differ between Tg-Capn2/tTA mice and their littermate controls at age 3 months; however, in Tg-Capn2/tTA mice, the levels of LC3BII and p62 were significantly elevated in the heart at age 6 months and further increased at age 12 months as compared to those at age 3 months (Fig. 2a), suggesting age-dependent over-induction of autophagy and/or blockage of autophagic flux. The aberrant autophagy was well correlated with the phenotypes of dilated cardiomyopathy in Tg-Capn2/tTA mice (Fig. 1), suggesting a potential role of aberrant autophagy.

To further address aberrant autophagy in hearts of Tg-Capn2/tTA mice, we conducted transmission electron microscopic analysis. After overnight fasting, Tg-Capn2/tTA mice at age 8 months had more autophagosomes in cardiomyocytes than those in their wild-type littermates, substantiating the presence of aberrant autophagy in Tg-Capn2/tTA mouse hearts (Fig. 2b).

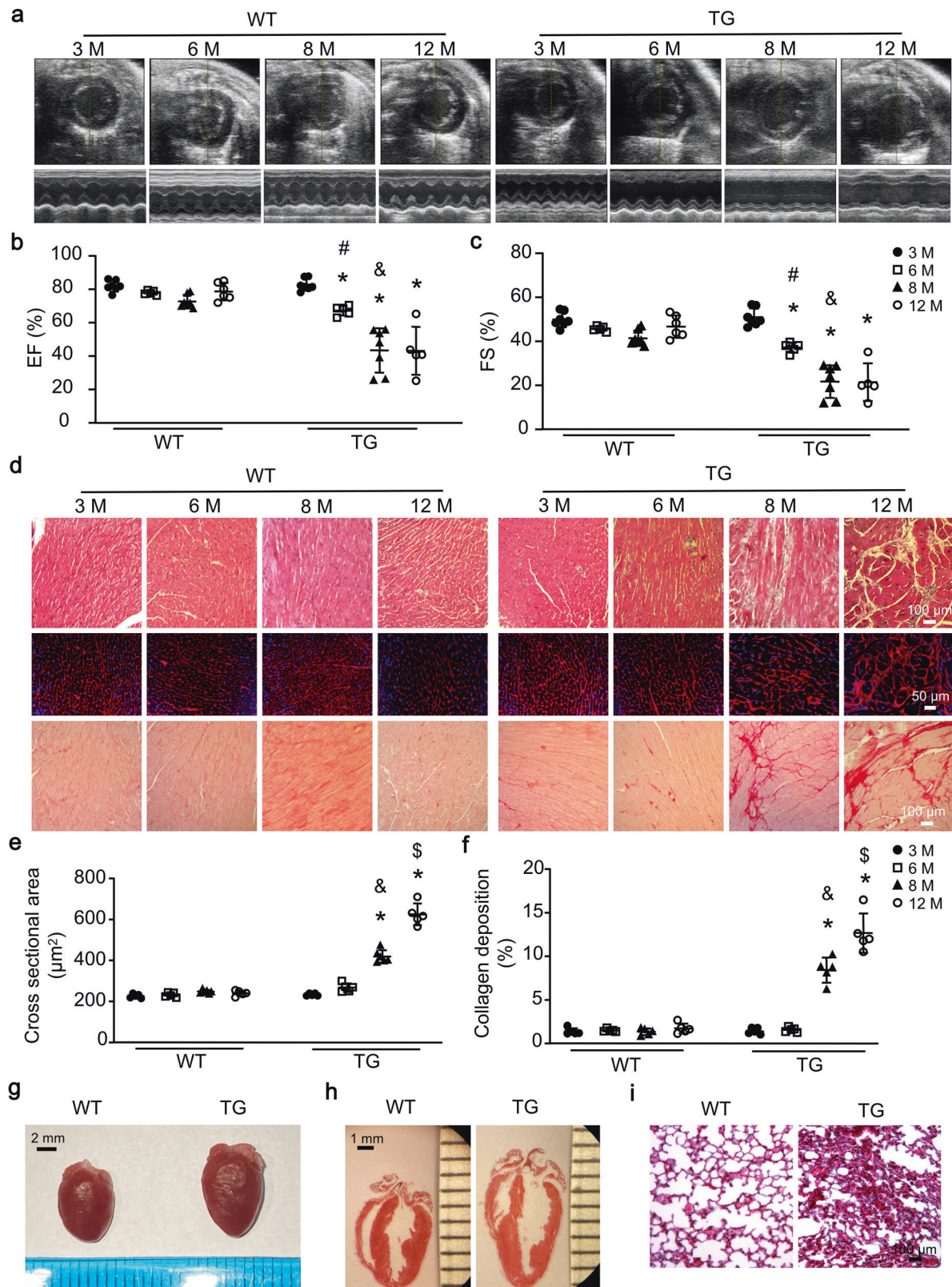


Fig. 1 Echocardiographic and histological analysis. Echocardiography was performed in Tg-Capn2/tTA mice (TG) and their littermate controls (WT) at ages 3, 6, 8 and 12 months. At the end of each experiment, heart tissues were collected for further analysis. **a** Echocardiographic analysis. Upper panel: representative B-mode images and lower panel: M-mode images. **b** Ejection fraction (EF%). **c** Fractional shortening (FS%). **d** A representative H&E, WGA and sirius red staining of heart tissues from mice at age 3, 6, 8 and 12 months. **e** Quantification for cardiomyocyte cross-sectional area. **f** Quantification for collagen deposition. **g, h** A representative picture of whole heart and H&E staining for heart chambers from mice at age 8 months. **i** A representative picture of H&E staining for lungs from mice at age 8 months. Data are mean \pm SD, $n = 5-7$. * $P < 0.05$ versus age-matched WT mice, # $P < 0.05$ versus TG mice at age 3 months, & $P < 0.05$ versus TG mice at age 6 months, and $\$P < 0.05$ versus TG mice at age 8 months.

Table 1. Echocardiographic analysis and body weight in mice.

Groups	LVID-s (mm)	LVID-d (mm)	LVAW-d (mm)	LVPW-d (mm)	Body weight (g)
Control + Vehicle	2.52 ± 0.27	4.17 ± 0.31	0.71 ± 0.07	0.76 ± 0.03	33.67 ± 3.07
Control + 3-MA	2.06 ± 0.31	3.76 ± 0.25	0.75 ± 0.07	0.81 ± 0.08	38.17 ± 5.25
Tg-Capn2/tTA + Vehicle	3.96 ± 0.68*	4.75 ± 0.40*	0.82 ± 0.09	0.83 ± 0.10	37.06 ± 5.12
Tg-Capn2/tTA + 3-MA	2.73 ± 0.51 [#]	4.00 ± 0.48 [#]	0.79 ± 0.11	0.79 ± 0.09	36.18 ± 9.19

Data are mean ± SD (*n* = 6–8). LVID-s indicates left ventricular systolic internal dimension, and LVID-d indicates left ventricular diastolic internal dimension. LVAW-d indicates left ventricle diastolic anterior wall thickness, and LVPW-d indicates left ventricle diastolic posterior wall thickness. **P* < 0.05 versus Control + Vehicle, and [#]*P* < 0.05 versus Tg-Capn2/tTA+Vehicle.

Over-expression of calpain-2 blocks autophagic flux in cultured cardiomyocytes

To provide further insight into aberrant autophagy induced by calpain-2, we infected neonatal mouse cardiomyocytes with Ad-Capn2 or Ad-HA. Three days later, infection of Ad-Capn2 resulted in much higher levels of CAPN2, LC3BII and p62 protein compared with Ad-HA infection (Fig. 2c), suggesting the possibility of impaired autophagic flux. To address this, we incubated cardiomyocytes with bafilomycin A1 for 2 h, an inhibitor of late stage of autophagy. Treatment of bafilomycin A1 induced a significant increase in the protein levels of LC3BII in Ad-HA infected cardiomyocytes. However, bafilomycin A1 did not further increase LC3BII protein levels in Ad-Capn2 infected cardiomyocytes (Fig. 2d), suggesting that the accumulation of LC3BII in Ad-Capn2 infected cardiomyocytes stems from inhibition of LC3BII turnover, implicating the blockage of autophagic flux. Since lysosomal dysfunction ensures autophagic flux blockage, we analyzed lysosomal pH value in cardiomyocytes as lysosome acidification is required for its function to degrade autolysosomes. Similar to bafilomycin A1, infection of Ad-Capn2 resulted in an elevation of pH value in cardiomyocytes compared with Ad-HA infection (Fig. 2e). Ad-Capn2-induced calpain-2 over-expression impaired lysosomal function as demonstrated by a reduction of mature cathepsin B protein in neonatal cardiomyocytes (Fig. 2f). To test this further, we determined lysosomal membrane permeability by lysosomal galectin puncta assay [32]. Accordingly, we infected H9c2 cells with Ad-hLGALS1/GFP followed by Ad-Capn2 or Ad-HA. Three days later, confocal fluorescence microscopy showed much more GFP-fluorescent LGALS1 puncta in the cytoplasm of Ad-Capn2 compared with Ad-HA infected H9c2 cells (Fig. 2g), indicating that calpain-2 over-expression increases the lysosomal membrane permeability.

Administration of 3-MA inhibits autophagy and reduces dilated cardiomyopathy in Tg-Capn2/tTA mice

Having shown that aberrant autophagy is correlated with development of dilated heart failure in transgenic Tg-Capn2/tTA mice, we hypothesized that inhibition of autophagy induction might alleviate calpain-2 induced dilated cardiomyopathy. To examine this hypothesis, we treated Tg-Capn2/tTA mice and their littermate controls with 3-MA, a well established inhibitor of class III phosphoinositide 3-kinase that prevents autophagy induction [33], or vehicle once every 3 days starting from age 6 months for a total of 2 months. This timeframe was chosen because Tg-Capn2/tTA mice began to display mild myocardial dysfunction at age 6 months and had severe myocardial dysfunction at age 8 months (Fig. 1a–c). Two months after 3-MA treatment, Tg-Capn2/tTA mice and their littermate controls had comparable body weight among 4 different groups without other health and behavior problems (Table 1). The protein levels of LC3BII and p62 were much higher in heart tissue lysates of Tg-Capn2/tTA mice relative to their littermate controls at age 8 months, which were prevented by 3-MA (Fig. 3a–c), indicating a successful inhibition of aberrant autophagy.

Echocardiographic analysis showed that myocardial function was decreased as indicated by a lower EF% and FS% in Tg-Capn2/tTA mice compared with their littermate controls at age 8 months after vehicle treatment. In contrast, myocardial function was relatively preserved in Tg-Capn2/tTA mice after 3-MA treatment for 2 months (Fig. 3d–f). As a serum biomarker of myocardial injury, troponin I level was elevated in Tg-Capn2/tTA mice compared with their littermate controls at age 8 months; however, administration of 3-MA significantly reduced the level of troponin I in Tg-Capn2/tTA mice (Fig. 3g). In line with myocardial injury, histological analysis revealed that administration of 3-MA reduced pathological scores in Tg-Capn2/tTA mouse hearts (Fig. 3h, i). These results suggest that inhibition of autophagy induction protects against calpain-2 over-expression induced heart injury.

An important feature of dilated cardiomyopathy is adverse myocardial remodeling including myocardial hypertrophy and interstitial fibrosis in the heart [34]. As shown in Fig. 4a, Tg-Capn2/tTA mice exhibited a higher ratio of heart weight to tibia length as compared to that of their wild-type littermates, which was reduced by 3-MA treatment. Similarly, 3-MA treatment resulted in a smaller cardiomyocyte cross-sectional area in Tg-Capn2/tTA mice (Fig. 4b, c). These results demonstrated that inhibition of autophagy induction reduced myocardial hypertrophy in Tg-Capn2/tTA mice. This was further supported by the evidence of hypertrophy-related gene expression. Transgenic over-expression of calpain-2 induced a significant up-regulation of ANP and β-MHC mRNA in Tg-Capn2/tTA mouse hearts compared with their littermate controls, which was attenuated by 3-MA treatment (Fig. 4d, e). To determine fibrosis, we analyzed collagen deposition in the heart. Collagen deposition in heart sections was much less in Tg-Capn2/tTA mice treated with 3-MA compared with vehicle (Fig. 4b, f). Furthermore, the mRNA levels of collagen-I and collagen-III were significantly higher in Tg-Capn2/tTA mice compared with their littermate controls, which were also prevented by administration of 3-MA (Fig. 4g, h).

Transgenic over-expression of calpain-2 induces a reduction of junctophilin-2 protein in Tg-Capn2/tTA mouse hearts which is attenuated by 3-MA

Our recent study reported that calpain-2 cleaved junctophilin-2 protein at the same site as calpain-1 [24]. Since a reduction of junctophilin-2 has been implicated in development of heart failure [35], we determined CAPN2 and junctophilin-2 protein in Tg-Capn2/tTA mouse hearts. As shown in Fig. 5a, Tg-Capn2/tTA mice exhibited a significant increase in CAPN2 protein levels in the heart at age 3 months, which was further increased at age 8 months. The protein levels of junctophilin-2 did not differ between Tg-Capn2/tTA mice and their wild-type littermates at age 3 months (Fig. 5b); however, at age 8 months, Tg-Capn2/tTA mice exhibited a reduction of junctophilin-2 protein and a concomitant increase in cleaved fragment of junctophilin-2 (around 75 kDa) in the heart as compared to that of their littermate controls (Fig. 5b, c). Administration of 3-MA relatively preserved the protein level of junctophilin-2 and reduced the cleaved fragment of junctophilin-2

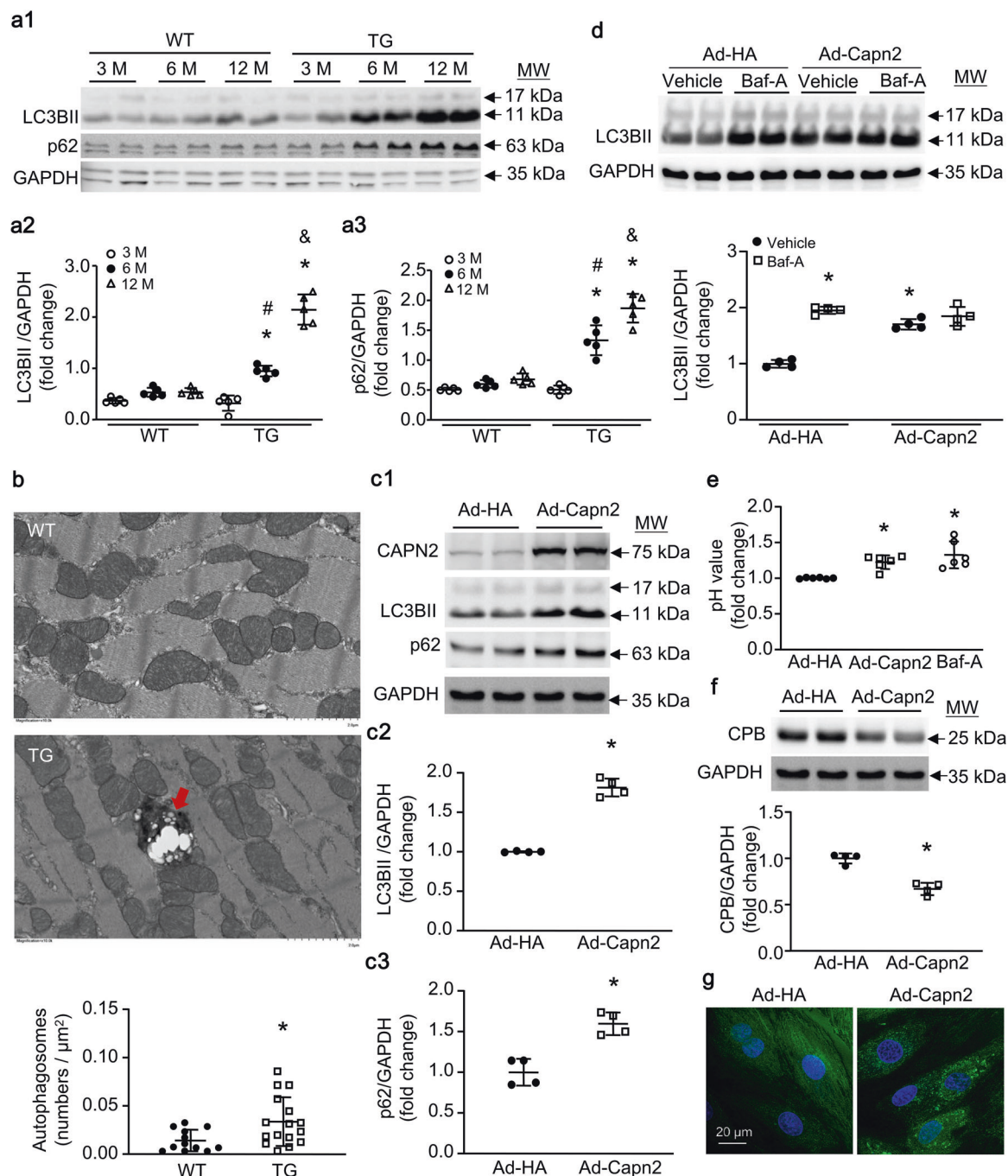


Fig. 2 Determination of autophagy activity. **a1** Representative Western blots for LC3BII and p62 in heart tissues from Tg-Capn2/tTA mice (TG) and their littermate controls (WT) at ages 3 months (3 M), 6 months (6 M) and 12 months (12 M). **a2** Quantification of LC3BII relative to GAPDH. **a3** Quantification of p62 relative to GAPDH. Data are mean \pm SD, $n = 5$. * $P < 0.05$ versus age-matched WT mice, # $P < 0.05$ versus TG mice at age 3 months, and & $P < 0.05$ versus TG mice at age 6 months. **b** Transmission electron microscopy (TEM) of heart tissues from TG and WT mice at age 8 months. Upper panel: Representative TEM images of cellular degradation machinery in heart muscles and lower panel: Quantification of the number of autophagosomes per square micron in TG and WT mouse hearts. Data are mean \pm SD. * $P < 0.05$. Red arrow points to autophagosome. **c–g** Neonatal mouse cardiomyocytes were infected with Ad-Capn2 or Ad-HA. Seventy-two hours later, Western blot analysis was conducted to determine the levels of LC3BII, p62 and GAPDH protein. **c1** Representative Western blots for CAPN2, LC3BII, p62 and GAPDH protein. **c2** Quantification of LC3BII/GAPDH and **(c3)** quantification of p62/GAPDH. **d** Autophagic flux assay. Seventy-two hours after adenoviral infection, cardiomyocytes were incubated with bafilomycin A (Baf-A, 100 nM) or Vehicle for 2 h. The levels of LC3BII and GAPDH were determined by Western blot analysis. Upper panel: Representative Western blots for LC3BII and GAPDH and lower panel: quantification of LC3BII/GAPDH. **e** Lysosomal pH value was determined. Baf-A served as a positive control. **f** Upper panel: representative Western blots for mature cathepsin B (CPB) and GAPDH. Lower panel: quantification of CPB/GAPDH. Data are mean \pm SD from 4–6 different cell cultures. * $P < 0.05$ versus Ad-HA or Ad-HA + Vehicle. **g** H9c2 cells were infected with Ad-hLgals1/GFP and then Ad-Capn2 or Ad-HA. Seventy-two hours later, confocal microscopy was conducted to visualize GFP-fused hLgals1. Nuclei were stained by Hoechst 33342. Representative confocal microscopic images from 3 different cell cultures show that Ad-Capn2 infection resulted in higher levels of GFP-fluorescent hLgals1 puncta in H9c2 cells. MW molecular weight.

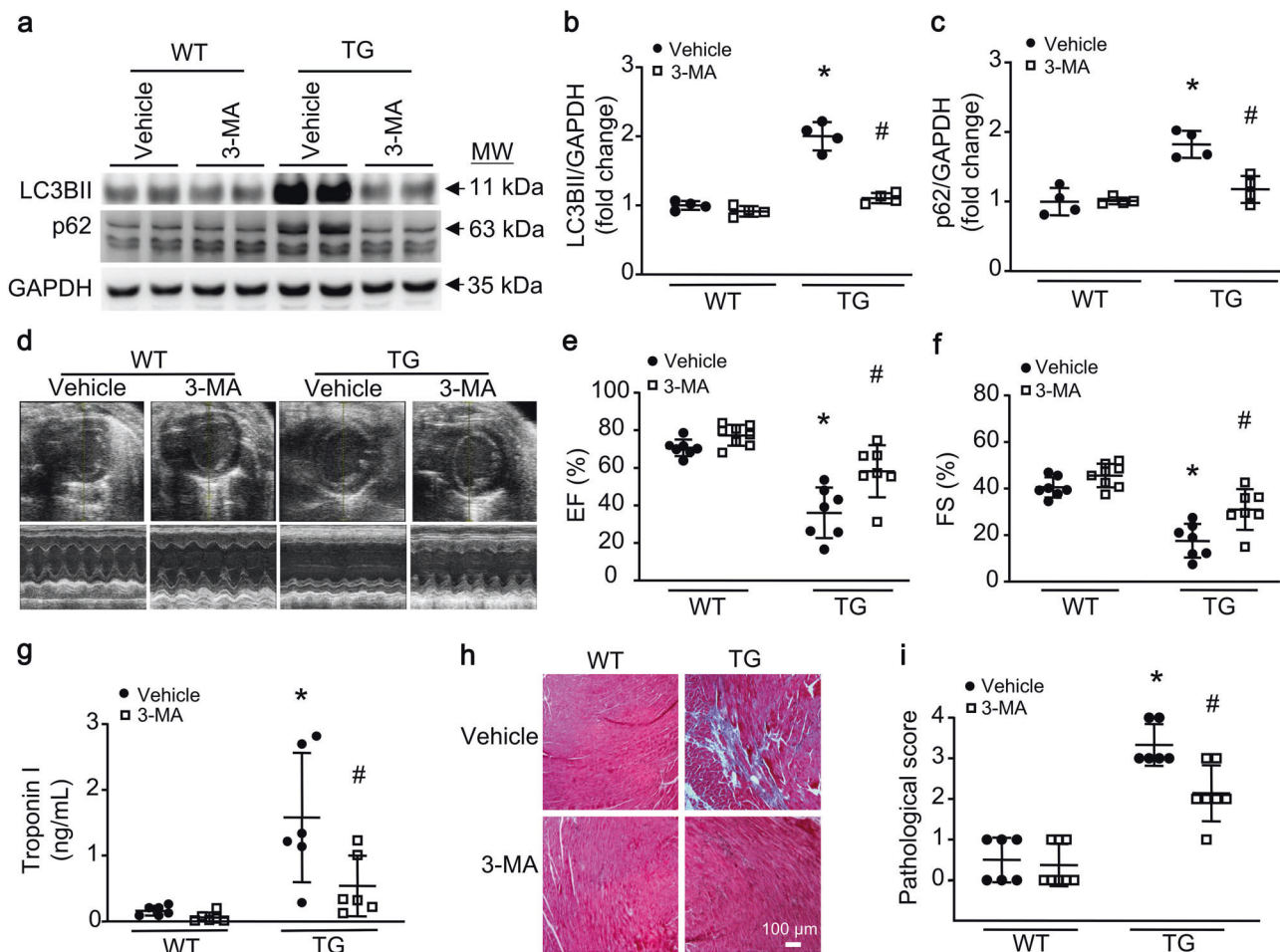


Fig. 3 Effects of 3-MA on autophagy activity, myocardial function and injury in Tg-Capn2/tTA mice. Tg-Capn2/tTA mice (TG) and their littermate controls (WT) were treated with 3-MA or Vehicle once every 3 days starting from age 6 months for a total of 2 months. **a** Representative Western blots for LC3BII and p62. **b, c** Quantification of LC3BII and p62 relative to GAPDH. **d–f** Echocardiographic analysis: representative B-mode (upper panel) and M-mode images (lower panel) (**d**), ejection fraction (EF%, **e**) and fractional shortening (FS%, **f**). **g** ELISA measurement of serum troponin I. **h, i** A representative H&E staining of heart tissues at age 8 months (**h**) and pathology scores (**i**). Data are mean \pm SD, $n = 4–7$. * $P < 0.05$ versus Vehicle + WT and # $P < 0.05$ versus Vehicle + TG. MW molecular weight.

in Tg-Capn2/tTA mouse hearts (Fig. 5c). This result suggests that sustained up-regulation of calpain-2 induces a reduction of junctophilin-2 in the heart, at least partly through aberrant autophagy. To address this, we infected neonatal cardiomyocytes with Ad-Capn2 or Ad-HA. Three days later, the protein levels of JPH2 were much lower whereas LC3BII levels were higher in Ad-Capn2 compared with Ad-HA infected cardiomyocytes. However, in the presence of 3-MA the protein levels of JPH2 and LC3BII did not differ between Ad-Capn2 and Ad-HA infected cardiomyocytes (Fig. 6a–c), indicating that calpain-2 reduces JPH2 protein levels through aberrant autophagy. Interestingly, the protein levels of JPH2 were not changed when autophagy was induced by rapamycin in cardiomyocytes (Fig. 6d, e). In contrast, incubation with bafilomycin A significantly reduced JPH2 protein levels while increasing LC3BII levels (Fig. 6d–f). Since we have shown that calpain-2 over-expression impaired autophagic flux (Fig. 2), these results argue that autophagic flux blockage mediates calpain-2 induced JPH2 reduction in cardiomyocytes.

DISCUSSION

Calpain activation has been implicated in heart diseases and may represent an important target for therapy [12, 15, 36, 37]. Increased calpain-1 was sufficient to induce cell death in cultured cardiomyocytes and dilated cardiomyopathy in transgenic mice

[4, 16] whereas knockdown of calpain-1 prevented cardiomyocyte death and reduced cardiac pathology under stress [5, 13, 36, 38]. Unlike calpain-1, increased calpain-2 was not sufficient to induce cell death in cultured cardiomyocytes and transgenic mice with cardiomyocyte-specific calpain-2 over-expression did not exhibit cardiac phenotypes by age 4 months [17]. This study provides the first evidence that sustained over-expression of calpain-2 in cardiomyocytes sufficiently induced age-dependent dilated cardiomyopathy in transgenic mice. This finding implies that aging may predispose the heart to calpain-2-induced injury, which has potential clinical relevance as heart diseases usually occur in aged patients and calpain-2 was reported to increase in diseased hearts from patients [39, 40] and animal models [41, 42]. Our finding also indicates that the transgenic Tg-Capn2/tTA mice may represent a useful mouse model of heart failure to examine the therapeutic effects of potential calpain-2 inhibitors and explore mechanisms of calpain-2 related heart failure.

The mechanisms by which sustained up-regulation of calpain-2 induced age-dependent dilated cardiomyopathy are currently unknown. However, our data suggest that aberrant autophagy may contribute to calpain-2-induced dilated cardiomyopathy in transgenic mice. This is supported by several lines of evidence. First, aberrant autophagy well correlated with the decline of heart function and cardiac pathological changes in transgenic Tg-Capn2/tTA mice from ages 3 to 12 months. Second, inhibition of autophagy

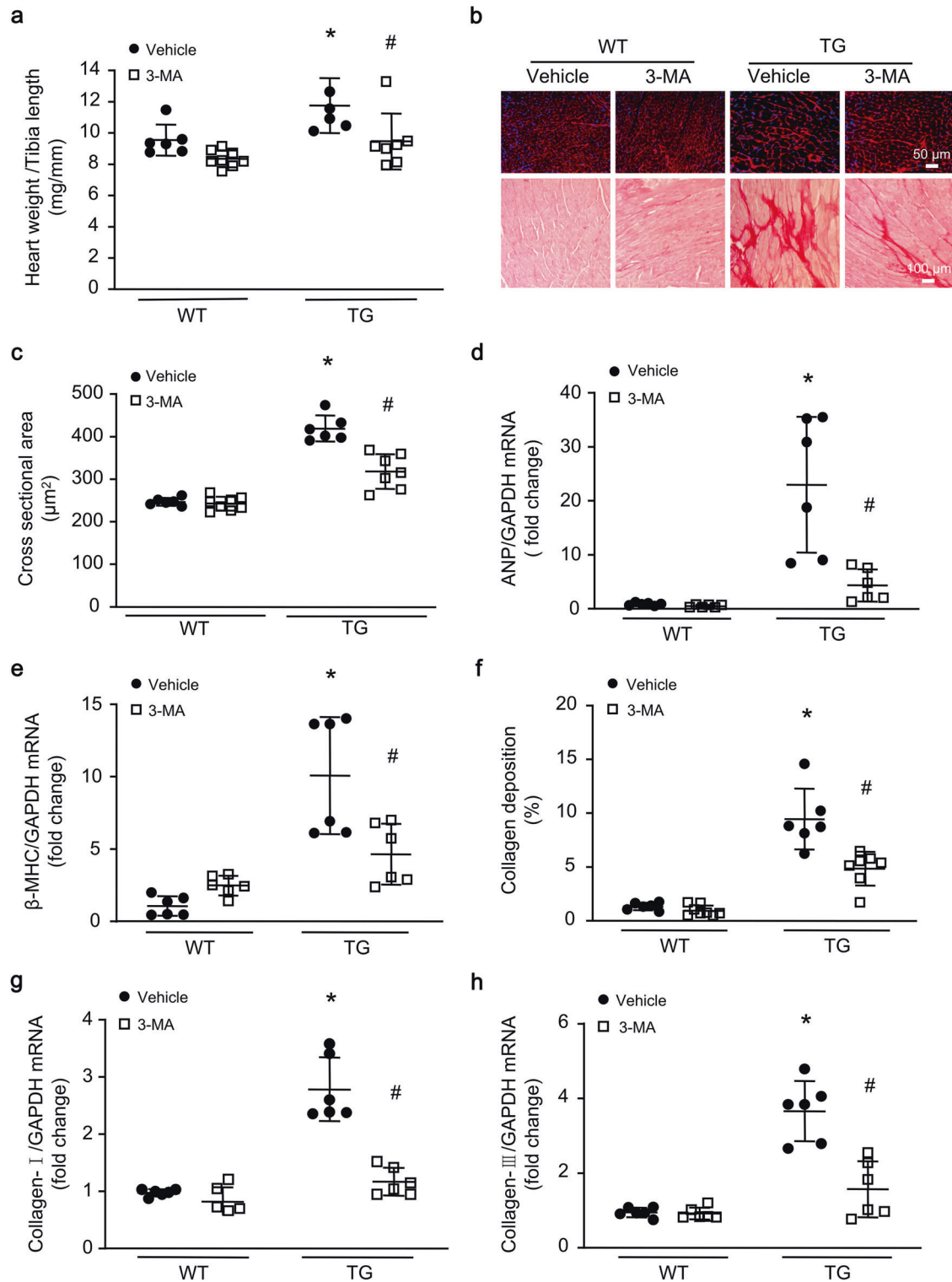


Fig. 4 Effects of 3-MA on cardiac hypertrophy and fibrosis in Tg-Capn2/tTA mice. Tg-Capn2/tTA mice (TG) and their littermate controls (WT) were injected with 3-MA or Vehicle once every 3 days starting from age 6 months for a total of 2 months. **a** Heart weight/Tibia length ratio (mg/mm). **b** A representative histological picture of WGA and sirius red staining. **c** Quantification for cardiomyocyte cross-sectional areas (μm²). The mRNA levels of ANP (**d**) and β-MHC (**e**) in heart tissues were analyzed by real-time RT-PCR. **f** Quantification for collagen deposition. The mRNA levels of collagen-I (**g**) and collagen-III (**h**) in heart tissues were determined by real-time RT-PCR. Data are mean ± SD, *n* = 6–7. **P* < 0.05 versus Vehicle + WT and #*P* < 0.05 versus Vehicle + TG.

induction with 3-MA reversed cardiac phenotypes in transgenic Tg-Capn2/tTA mice. Third, the presence of cardiac phenotypes in Tg-Capn2/tTA mice was closely associated with an increase in p62 and accumulation of autophagosomes, indicative of impaired

autophagic flux activity. Fourth, autophagic flux assay using bafilomycin A confirmed autophagic flux blockage in cardiomyocytes with calpain-2 over-expression. While autophagic activity is essential for cardiac homeostasis by degrading misfolded proteins,

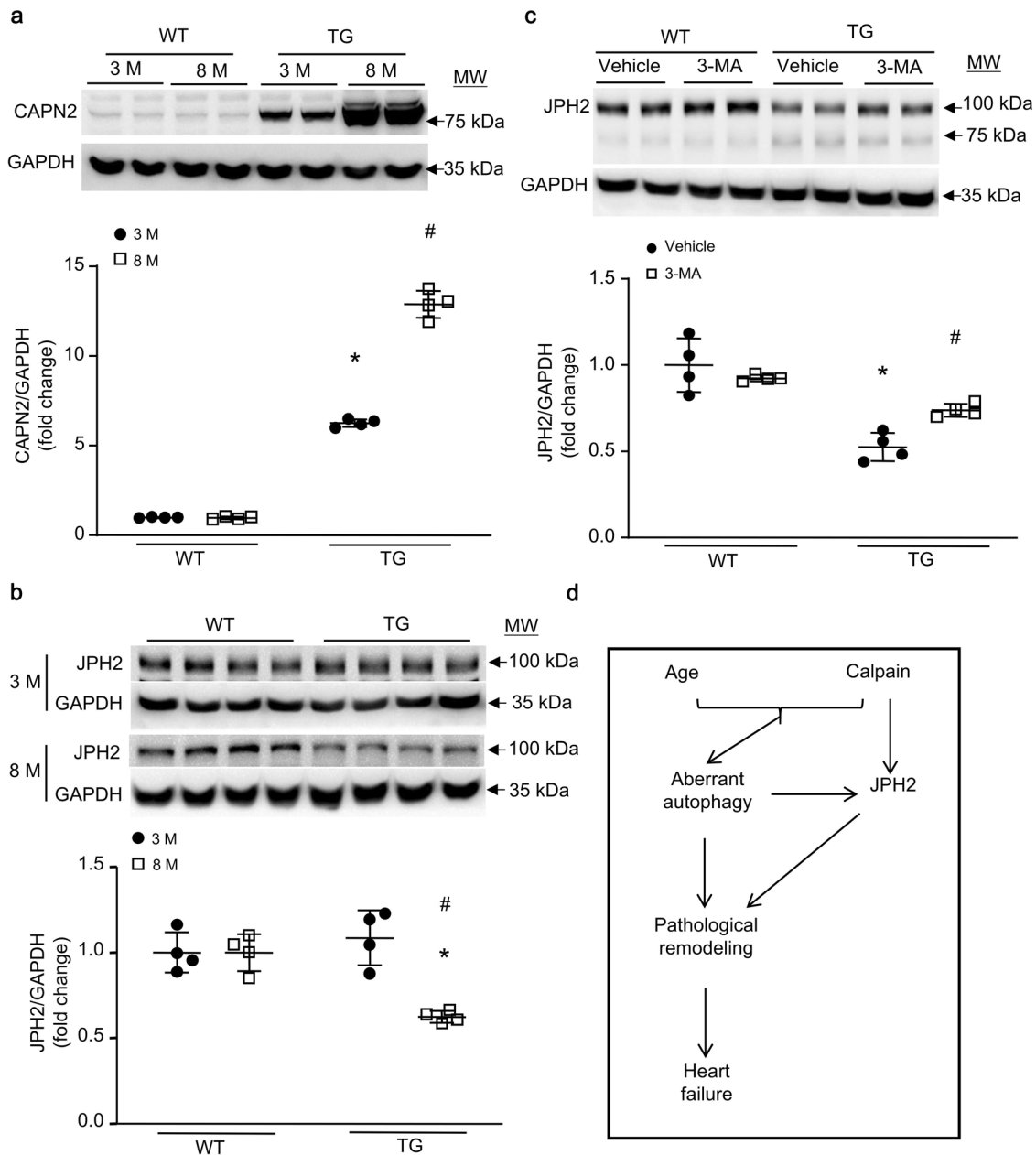


Fig. 5 Determination of junctophilin-2 (JPH2) protein expression in heart tissues. **a** The protein levels of CAPN2 and GAPDH were determined by Western blot analysis in Tg-Capn2/tTA mice (TG) and their littermate controls (WT). Upper panel: Representative Western blots for CAPN2 and GAPDH in heart tissues from mice at ages 3 and 8 months (3 M and 8 M), and bottom panel: quantification of CAPN2 protein levels relative to GAPDH. Data are mean \pm SD, $n = 4$. * $P < 0.05$ versus WT (3 M) and # $P < 0.05$ versus TG (3 M). **b** Upper panel: a representative Western blot for JPH2 in heart tissues from mice at ages 3 M and 8 M, and bottom panel: quantification of JPH2 protein levels relative to GAPDH. Data are mean \pm SD, $n = 4$. * $P < 0.05$ versus WT (8 M) and # $P < 0.05$ versus TG (3 M). **c** TG and WT mice were injected with 3-MA or Vehicle once every 3 days starting from age 6 months for a total of 2 months. Upper panel: a representative Western blot for JPH2 in heart tissues and bottom panel: quantification of JPH2 relative to GAPDH. Data are mean \pm SD, $n = 4$. * $P < 0.05$ versus Vehicle + WT and # $P < 0.05$ versus Vehicle + TG. **d** Diagram showing that increased calpain-2 together with age induces aberrant autophagy which damages the heart and reduces JPH2 protein through aberrant autophagy and direct cleavage, both of which contribute to pathological remodeling and heart failure. MW molecular weight.

damaged organelles and other macromolecules in a lysosome-dependent way, allowing for the recycling of cellular components [43, 44], dysfunctional autophagy including over-induction of autophagy and impaired autophagic flux has been contributing to cardiomyocyte injury and death under pathological conditions [44, 45]. Thus, our data implicated over-induction of autophagy and/or impaired autophagic flux in sustained calpain-2 over-expression-induced dilated cardiomyopathy. In this regard, inhibition of calpain

was reported to prevent Coxsackivirus B3-induced autophagy in H9c2 cardiomyocytes and protect lysosomal integrity and autophagic flux activity in *Pkd1*-deficient cells [46]. A recent study also showed that calpain-2 mediated TNF- α -induced autophagy in mouse hippocampal neurons [47]. Although the molecular mechanisms by which calpain-2 impairs autophagic flux remain unclear in cardiac pathology, our data suggest that calpain-2 may damage lysosomal function thereby blocking autophagic flux.

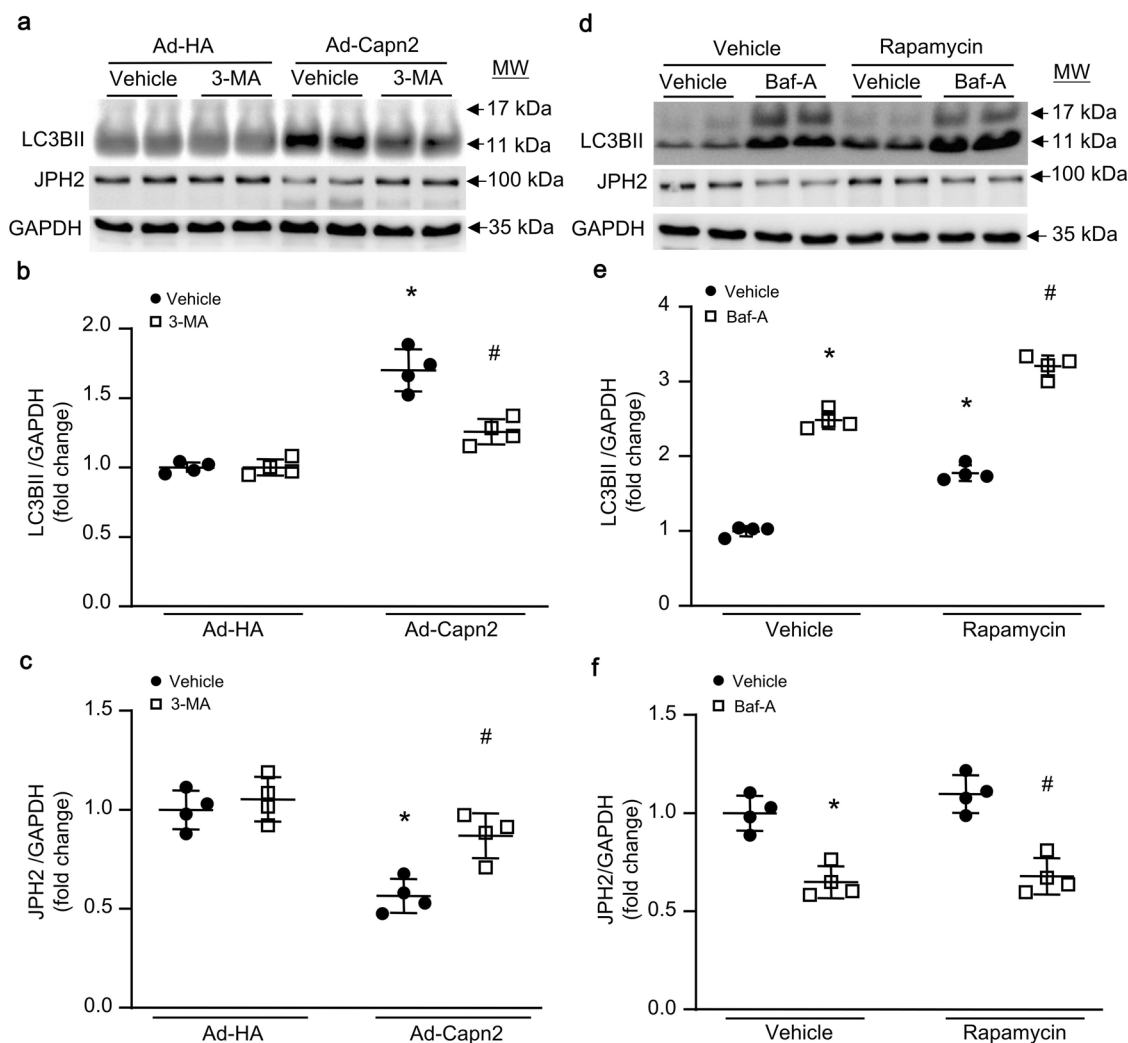


Fig. 6 Modulation of JPH2 protein levels by calpain-2 induced autophagy. **a–c** Neonatal mouse cardiomyocytes were infected with Ad-Capn2 or Ad-HA and then incubated with 3-MA (500 μ M) or Vehicle for 72 h. **a** Representative Western blots for LC3BII, JPH2 and GAPDH. **b** Quantification of LC3BII/GAPDH. **c** Quantification of JPH2/GAPDH. Data are mean \pm SD, $n = 4$ different cell cultures. * $P < 0.05$ versus Ad-HA + Vehicle and # $P < 0.05$ versus Ad-Capn2 + Vehicle. **d–f** Neonatal mouse cardiomyocytes were incubated with rapamycin (10 μ M) or Vehicle in combination with bafilomycin A (Baf-A, 100 nM) for 24 h. **d** Representative Western blots for LC3BII, JPH2 and GAPDH. **e** Quantification of LC3BII/GAPDH. **f** Quantification of JPH2/GAPDH. Data are mean \pm SD, $n = 4$ different cell cultures. * $P < 0.05$ versus Vehicle + Vehicle and # $P < 0.05$ versus Rapamycin + Vehicle. MW molecular weight.

We recently reported that calpain-2 cleaved junctophilin-2 [24]. Consistently, this study showed that the protein level of junctophilin-2 was reduced in transgenic Tg-Capn2/tTA mouse hearts, which correlated with an increase in a calpain-1/2 dependent cleaved fragment of junctophilin-2 [24]. A reduction of junctophilin-2 has been associated with hypertrophic cardiomyopathy [48] and heart failure [49], and over-expression of junctophilin-2 was reported to mitigate the progression of heart failure [50, 51]. Therefore, it is possible that decreased junctophilin-2 may be one of potential mechanisms in calpain-2-induced age-dependent cardiomyopathy. Interestingly, inhibition of autophagy with 3-MA increased the protein level of junctophilin-2 in transgenic Tg-Capn2/tTA mouse hearts, suggesting that in addition to direct proteolysis of junctophilin-2, calpain-2 may also indirectly regulate junctophilin-2 protein expression in the heart through an unappreciated autophagy-dependent mechanism. Our study further demonstrated that calpain-2-induced blockage of autophagic flux accounts for junctophilin-2 reduction in cardiomyocytes.

It is worthwhile to mention that transgenic calpain-2 expression increased with age in the heart. This raised such possibility that the

protein level of transgenic calpain-2 was not high enough to cause damage to the heart in Tg-Capn2/tTA mice when they are young (before age 3 months). However, this is unlikely because calpain-2 is expressed abundantly in cardiomyocytes under normal conditions and adenoviral vector-mediated calpain-2 over-expression at a level comparable to that observed in Tg-Capn2/tTA mice did not induce damage in cultured cardiomyocytes [17, 19].

In summary, we have provided direct evidence revealing that sustained over-expression of calpain-2 induces age-dependent dilated cardiomyopathy in mice, which may be mediated through aberrant autophagy and down-regulation of junctophilin-2 protein (Fig. 5d). Thus, a sustained increase in calpain-2 may be detrimental to the heart.

AUTHOR CONTRIBUTIONS

GCF, LSS, ZLS and TQP designed the research; XYJ, DZ, RN, JXW, JQS, ZV and AH performed the research; XYJ, DZ, RN, JXW, JQS, ZV and AH analyzed the data; XYJ, ZLS and TQP wrote the paper; GCF, LSS, SC and TQP discussed and revised the paper. All authors approved the present form of the paper.

FUNDING

This study was supported by the Doctorial Innovation Projects of Jiangsu Province (Grant No. KYCX17_1816 to XYJ), the Natural Sciences and Engineering Research Council of Canada (RGPIN-2017-04768 to TQP), the Heart & Stroke Foundation of Canada (G-17-0018361 to TQP), the Lawson Internal Research Fund, and Projects of International Cooperation from Jiangsu (BX2019100) and International Cooperation and Exchange from Zhenjiang (GJ2020010).

ADDITIONAL INFORMATION

Supplementary information The online version contains supplementary material available at <https://doi.org/10.1038/s41401-022-00965-9>.

Competing interests: The authors declare no competing interests.

REFERENCES

- Goll DE, Thompson VF, Li H, Wei W, Cong J. The calpain system. *Physiol Rev.* 2003;83:731–801.
- Sorimachi H, Ono Y. Regulation and physiological roles of the calpain system in muscular disorders. *Cardiovasc Res.* 2012;96:11–22.
- Ma J, Wei M, Wang Q, Li J, Wang H, Liu W, et al. Deficiency of Capn4 gene inhibits nuclear factor- κ B (NF- κ B) protein signaling/inflammation and reduces remodeling after myocardial infarction. *J Biol Chem.* 2012;287:27480–9.
- Zheng D, Wang G, Li S, Fan GC, Peng T. Calpain-1 induces endoplasmic reticulum stress in promoting cardiomyocyte apoptosis following hypoxia/reoxygenation. *Biochim Biophys Acta.* 2015;1852:882–92.
- Li S, Zhang L, Ni R, Cao T, Zheng D, Xiong S, et al. Disruption of calpain reduces lipotoxicity-induced cardiac injury by preventing endoplasmic reticulum stress. *Biochim Biophys Acta.* 2016;1862:2023–33.
- Ni R, Zheng D, Xiong S, Hill DJ, Sun T, Gardiner RB, et al. Mitochondrial calpain-1 disrupts ATP synthase and induces superoxide generation in type 1 diabetic hearts: A novel mechanism contributing to diabetic cardiomyopathy. *Diabetes.* 2016;65:255–68.
- Takano J, Mihira N, Fujioka R, Hosoki E, Chishti AH, Saido TC. Vital role of the calpain-calpastatin system for placental-integrity-dependent embryonic survival. *Mol Cell Biol.* 2011;31:4097–106.
- Dutt P, Croall DE, Arthur JS, Veyra TD, Williams K, Elce JS, et al. m-Calpain is required for preimplantation embryonic development in mice. *BMC Dev Biol.* 2006;6:3–13.
- Chen Q, Paillard M, Gomez L, Ross T, Hu Y, Xu A, et al. Activation of mitochondrial μ -calpain increases AIF cleavage in cardiac mitochondria during ischemia-reperfusion. *Biochem Biophys Res Commun.* 2011;415:533–8.
- Shintani-Ishida K, Yoshida K. Mitochondrial m-calpain opens the mitochondrial permeability transition pore in ischemia-reperfusion. *Int J Cardiol.* 2015;197:26–32.
- Kudo-Sakamoto Y, Akazawa H, Ito K, Takano J, Yano M, Yabumoto C, et al. Calpain-dependent cleavage of N-cadherin is involved in the progression of post-myocardial infarction remodeling. *J Biol Chem.* 2014;289:19408–19.
- Ni R, Zheng D, Wang Q, Yu Y, Chen R, Sun T, et al. Deletion of capn4 protects the heart against endotoxemic injury by preventing ATP synthase disruption and inhibiting mitochondrial superoxide generation. *Circ Heart Fail.* 2015;8:988–96.
- Li X, Li Y, Shan L, Shen E, Chen R, Peng T. Over-expression of calpastatin inhibits calpain activation and attenuates myocardial dysfunction during endotoxaemia. *Cardiovasc Res.* 2009;83:72–9.
- Cao Y, Wang Q, Liu C, Wang W, Lai S, Zou H, et al. Capn4 aggravates angiotensin II-induced cardiac hypertrophy by activating the IGF-AKT signaling pathway. *J Biochem.* 2021;171:53–61.
- Wang Y, Chen B, Huang CK, Guo A, Wu J, Zhang X, et al. Targeting calpain for heart failure therapy: Implications from multiple murine models. *JACC Basic Transl Sci.* 2018;3:503–17.
- Cao T, Fan S, Zheng D, Wang G, Yu Y, Chen R, et al. Increased calpain-1 in mitochondria induces dilated heart failure in mice: role of mitochondrial superoxide anion. *Basic Res Cardiol.* 2019;114:17–31.
- Zheng D, Su Z, Zhang Y, Ni R, Fan GC, Robbins J, et al. Calpain-2 promotes MKP-1 expression protecting cardiomyocytes in both in vitro and in vivo mouse models of doxorubicin-induced cardiotoxicity. *Arch Toxicol.* 2019;93:1051–65.
- Sheng JJ, Chang H, Yu ZB. Nuclear translocation of calpain-2 mediates apoptosis of hypertrophied cardiomyocytes in transverse aortic constriction rat. *J Cell Physiol.* 2015;230:2743–54.
- Liu ZF, Ji JJ, Zheng D, Su L, Peng T. Calpain-2 protects against heat stress-induced cardiomyocyte apoptosis and heart dysfunction by blocking p38 mitogen-activated protein kinase activation. *J Cell Physiol.* 2019;234:10761–70.
- Chang H, Sheng JJ, Zhang L, Yue ZJ, Jiao B, Li JS, et al. ROS-induced nuclear translocation of calpain-2 facilitates cardiomyocyte apoptosis in tail-suspended rats. *J Cell Biochem.* 2015;116:2258–69.
- Aluja D, Inerte J, Penela P, Ramos P, Ribas C, Iñiguez M, et al. Calpains mediate isoproterenol-induced hypertrophy through modulation of GRK2. *Basic Res Cardiol.* 2019;114:21–36.
- Chen Q, Thompson J, Hu Y, Dean J, Lesnfsky EJ. Inhibition of the ubiquitous calpains protects complex I activity and enables improved mitophagy in the heart following ischemia-reperfusion. *Am J Physiol Cell Physiol.* 2019;317:C910–21.
- Zuo S, Kong D, Wang C, Liu J, Wang Y, Wan Q, et al. CRTH2 promotes endoplasmic reticulum stress-induced cardiomyocyte apoptosis through m-calpain. *EMBO Mol Med.* 2018;10:e8237–53.
- Wang J, Ciampa G, Zheng D, Shi Q, Chen B, Abel ED, et al. Calpain-2 specifically cleaves Junctophilin-2 at the same site as Calpain-1 but with less efficacy. *Biochem J.* 2021;478:3539–53.
- Sanbe A, Gulick J, Hanks MC, Liang Q, Osinska H, Robbins J. Reengineering inducible cardiac-specific transgenesis with an attenuated myosin heavy chain promoter. *Circ Res.* 2003;92:609–16.
- Li J, Zhu H, Shen E, Wan L, Arnold JM, Peng T. Deficiency of rac1 blocks NADPH oxidase activation, inhibits endoplasmic reticulum stress, and reduces myocardial remodeling in a mouse model of type 1 diabetes. *Diabetes.* 2010;59:2033–42.
- Garza-Lopez E, Vue Z, Katti P, Neikirk K, Biete M, Lam J, et al. Protocols for generating surfaces and measuring 3D organelle morphology using amira. *Cells.* 2021;11:65–80.
- Lam J, Katti P, Biete M, Mungai M, AshShareef S, Neikirk K, et al. A universal approach to analyzing transmission electron microscopy with ImageJ. *Cells.* 2021;10:2177–93.
- Peng T, Lu X, Lei M, Feng Q. Endothelial nitric-oxide synthase enhances lipopolysaccharide-stimulated tumor necrosis factor- α expression via cAMP-mediated p38 MAPK pathway in cardiomyocytes. *J Biol Chem.* 2003;278:8099–105.
- Demarchi F, Bertoli C, Copetti T, Tanida I, Brancolini C, Eskelinen EL, et al. Calpain is required for macroautophagy in mammalian cells. *J Cell Biol.* 2006;175:595–605.
- Demarchi F, Bertoli C, Copetti T, Eskelinen EL, Schneider C. Calpain as a novel regulator of autophagosome formation. *Autophagy.* 2007;3:235–7.
- Aits S, Krickler J, Liu B, Ellegaard AM, Hamalisto S, Tvingsholm S, et al. Sensitive detection of lysosomal membrane permeabilization by lysosomal galectin puncta assay. *Autophagy.* 2015;11:1408–24.
- Wu YT, Tan HL, Shui G, Bauvy C, Huang Q, Wenk MR, et al. Dual role of 3-methyladenine in modulation of autophagy via different temporal patterns of inhibition on class I and III phosphoinositide 3-kinase. *J Biol Chem.* 2010;285:10850–61.
- Dilated cardiomyopathy. *Nat Rev Dis Primers.* 2019;5:33.
- Guo A, Hall D, Zhang C, Peng T, Miller JD, Kutschke W, et al. Molecular determinants of calpain-dependent cleavage of junctophilin-2 protein in cardiomyocytes. *J Biol Chem.* 2015;290:17946–55.
- Li Y, Feng Q, Arnold M, Peng T. Calpain activation contributes to hyperglycaemia-induced apoptosis in cardiomyocytes. *Cardiovasc Res.* 2009;84:100–10.
- Thompson J, Hu Y, Lesnfsky EJ, Chen Q. Activation of mitochondrial calpain and increased cardiac injury: beyond AIF release. *Am J Physiol Heart Circ Physiol.* 2016;310:H376–84.
- Li Y, Ma J, Zhu H, Singh M, Hill D, Greer PA, et al. Targeted inhibition of calpain reduces myocardial hypertrophy and fibrosis in mouse models of type 1 diabetes. *Diabetes.* 2011;60:2985–94.
- Zhao Y, Cui GM, Zhou NN, Li C, Zhang Q, Sun H, et al. Calpain-calcineurin-nuclear factor signaling and the development of atrial fibrillation in patients with valvular heart disease and diabetes. *J Diabetes Res.* 2016;2016:4639654–60.
- Lahiri SK, Quick AP, Samson-Couterie B, Hulsurkar M, Elzenaar I, van Oort RJ, et al. Nuclear localization of a novel calpain-2 mediated junctophilin-2 C-terminal cleavage peptide promotes cardiomyocyte remodeling. *Basic Res Cardiol.* 2020;115:49–61.
- Takahashi M, Tanonaka K, Yoshida H, Oikawa R, Koshimizu M, Daicho T, et al. Effects of ACE inhibitor and AT1 blocker on dystrophin-related proteins and calpain in failing heart. *Cardiovasc Res.* 2005;65:356–65.
- Zhang K, Cremers MM, Wiedemann S, Poitz DM, Pfluecke C, Heinzel FR, et al. Spatio-temporal regulation of calpain activity after experimental myocardial infarction in vivo. *Biochem Biophys Res Commun.* 2021;28:101162–70.
- Shirakabe A, Zhai P, Ikeda Y, Saito T, Maejima Y, Hsu CP, et al. Drp1-dependent mitochondrial autophagy plays a protective role against pressure overload-induced mitochondrial dysfunction and heart failure. *Circulation.* 2016;133:1249–63.
- Matsui Y, Takagi H, Qu X, Abdellatif M, Sakoda H, Asano T, et al. Distinct roles of autophagy in the heart during ischemia and reperfusion: roles of AMP-activated protein kinase and Beclin 1 in mediating autophagy. *Circ Res.* 2007;100:914–22.
- Ma X, Liu H, Foyil SR, Godar RJ, Weinheimer CJ, Hill JA, et al. Impaired autophagosome clearance contributes to cardiomyocyte death in ischemia/reperfusion injury. *Circulation.* 2012;125:3170–81.
- Li M, Wang X, Yu Y, Xie Y, Zou Y, Ge J, et al. Coxsackievirus B3-induced calpain activation facilitates the progeny virus replication via a likely mechanism related

- with both autophagy enhancement and apoptosis inhibition in the early phase of infection: an in vitro study in H9c2 cells. *Virus Res.* 2014;179:177–86.
47. Li Y, He Z, Lv H, Chen W, Chen J. Calpain-2 plays a pivotal role in the inhibitory effects of propofol against TNF- α -induced autophagy in mouse hippocampal neurons. *J Cell Mol Med.* 2020;24:9287–99.
 48. Landstrom AP, Kellen CA, Dixit SS, van Oort RJ, Garbino A, Weisleder N, et al. Junctophilin-2 expression silencing causes cardiocyte hypertrophy and abnormal intracellular calcium-handling. *Circ Heart Fail.* 2011;4:214–23.
 49. Wei S, Guo A, Chen B, Kutschke W, Xie YP, Zimmerman K, et al. T-tubule remodeling during transition from hypertrophy to heart failure. *Circ Res.* 2010;107:520–31.
 50. Guo A, Zhang X, Iyer VR, Chen B, Zhang C, Kutschke WJ, et al. Overexpression of junctophilin-2 does not enhance baseline function but attenuates heart failure development after cardiac stress. *Proc Natl Acad Sci USA.* 2014;111:12240–5.
 51. Reynolds JO, Quick AP, Wang Q, Beavers DL, Philippen LE, Showell J, et al. Junctophilin-2 gene therapy rescues heart failure by normalizing RyR2-mediated Ca. *Int J Cardiol.* 2016;225:371–80.

Springer Nature or its licensor holds exclusive rights to this article under a publishing agreement with the author(s) or other rightsholder(s); author self-archiving of the accepted manuscript version of this article is solely governed by the terms of such publishing agreement and applicable law.